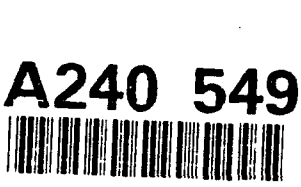

PL-TR-91-2074

AIRCRAFT LIDAR SENSITIVITY STUDY FOR MEASURING WATER VAPOR

R. J. Rieder
O. Shepherd

Visidyne, Inc
10 Corporate Place
South Bedford Street
Burlington, MA 01803

1 April 1991

Scientific Report No. 1

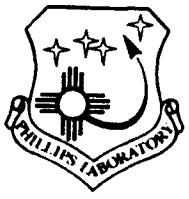

PHILLIPS LABORATORY
AIR FORCE SYSTEMS COMMAND
HANSCOM AIR FORCE BASE, MASSACHUSETTS 01731-5000

This technical report has been reviewed and is approved for publication.

DEAN F. KIMBALL
Contract Manager
Simulation Branch

DONALD E. BEDO, Chief
Electro-Optical Measurements Branch
Optical Environment Division

ALAN D. BLACKBURN, Col, USAF, Director
Optical Environment Division

This document has been reviewed by the ESD Public Affairs Office (PA) and is releasable to the National Technical Information Service (NTIS).

Qualified requestors may obtain additional copies from the Defense Technical Information Center. All others should apply to the National Technical Information Service.

If your address has changed, or if you wish to be removed from the mailing list, or if the addressee is no longer employed by your organization, please notify PL/IMA, Hanscom AFB, MA 01731-5000. This will assist us in maintaining a current mailing list.

REPORT DOCUMENTATION PAGE

Form Approved
OMB No 0704-0188

1. AGENCY USE ONLY (Leave blank)	2. REPORT DATE	3. REPORT TYPE AND DATES COVERED
	1 April 1991	Scientific Report No. 1

4. TITLE AND SUBTITLE
Aircraft Lidar Sensitivity Study for Measuring Water Vapor

5. FUNDING NUMBERS
PE 62101F
PR 3054 TA 01 WU A1
Contract F19628-88-C-0013

6. AUTHOR(S)
R.J. Rieder
O. Shepherd

7. PERFORMING ORGANIZATION NAME(S) AND ADDRESS(ES)
Visidyne, Inc.
10 Corporate Place
South Bedford Street
Burlington, MA 01803

8. PERFORMING ORGANIZATION REPORT NUMBER

9. SPONSORING/MONITORING AGENCY NAME(S) AND ADDRESS(ES)
Phillips Laboratory
Hanscom AFB, MA 01803

Contract Manager: Dean Kimball/OPS

10. SPONSORING/MONITORING AGENCY REPORT NUMBER
PL-TR-91-2074

11. SUPPLEMENTARY NOTES

12a. DISTRIBUTION/AVAILABILITY STATEMENT
Approved for public release; distribution unlimited.

12b. DISTRIBUTION CODE

13. ABSTRACT *(Maximum 200 words)*

The amount of water in the optical path between an airborne measurement platform and a target is responsible for the difference between the actual and the measurement target spectral radiance. In situ measurements of water vapor can be limited by outgassing from the sensor and/or its environment. A study was performed to investigate the use of lidar remote sensing techniques for the remote measurement of water vapor from a measurement aircraft such as the FISTA NKC-135A.

14. SUBJECT TERMS		15. NUMBER OF PAGES
Aircraft	Water Vapor	32
Lidar		16. PRICE CODE
Remote Sensing		

17. SECURITY CLASSIFICATION OF REPORT	18. SECURITY CLASSIFICATION OF THIS PAGE	19. SECURITY CLASSIFICATION OF ABSTRACT	20. LIMITATION OF ABSTRACT
Unclassified	Unclassified	Unclassified	SAR

TABLE OF CONTENTS

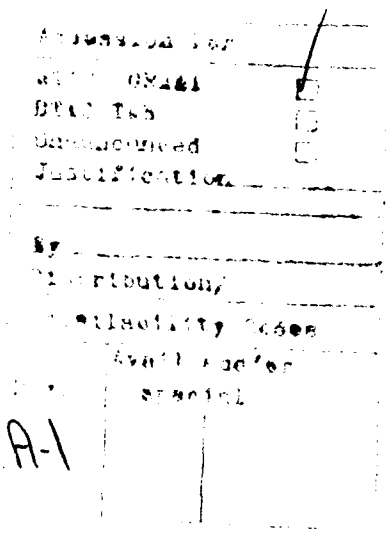

LIST OF FIGURES

Introduction

The amount of water in the optical path between an airborne measurement platform and a target is responsible for the difference between the actual and the measured target spectral radiance. In situ measurements of water vapor can be limited by outgassing from the sensor and/or its environment. The objective of this study was to investigate the use of lidar remote sensing techniques for the remote measurement of water vapor from a measurement aircraft such as the FISTA NKC-135A.

This report is a brief study of the signals anticipated in measuring the water vapor concentration in the troposphere from a lidar flown on an aircraft. Two detection mechanisms have been examined: conventional Raman scattering and differential absorption.

The basic lidar equation is

$$P_{rcl} = P_o \epsilon \beta e^{-\tau} A \delta r/r^2$$

where
- P_o = incident laser signal
- ϵ = system efficiency
- $e^{-\tau}$ = atmospheric transmission
- β = backscatter coefficient
- A = collecting area
- δr = size of atmospheric cell probed
- r = range

The two methods of detection are significantly different in approach. Raman scattering focuses on the backscatter coefficient, β, to obtain specie dependent information. The differential absorption technique is independent of the scattering mechanism and obtains the information from the extinction term, $e^{-\tau}$.

In both cases the laser beam is scattered 180 degrees back to the receiver. Fig. 1. shows the ratio of $\beta_{aerosol}/\beta_{rayleigh}$ for different wavelengths as a function of altitude. Backscatter from

aerosols dominate for the first 7 km whereas the Rayleigh scattering is responsible for scattering between the altitudes of 7 and 15 kilometers. These data have been fit to a polynomial and are extrapolated linearly for wavelengths greater than 1 μm.

Water Vapor in the Troposphere

The concentration of water vapor in the troposphere varies by over a factor of 10000. The mixing ratio (ppmv) decreases from 7750 ppmv at sea level to 5 ppmv at 15 km and remains essentially constant through out the stratosphere and mesosphere. The corresponding number density of water molecules is $2x10^{23}$ m^{-3} and $2x10^{19}$ m^{-3} at sea level and 15 km, respectively. Fig. 2. shows a plot of the water vapor density as a function of altitude over these altitudes.

Optical System

The calculations in this report were made assuming a coaxial lidar system in order to utilize the entire near field. In addition, the collecting optic is assumed to have a 7 inch diameter (248 cm^2) collecting mirror. The optics are assumed to consist of the aircraft window, a telescope, a filter and lens, and detector. Below is a list of the efficiencies used for the following set of calculations

Optical Efficiencies

Aircraft Window (Trans)	0.90
Aircraft Window (Rec)	0.90
Telescope	0.90
Filter	0.50
Lens	0.90
PMT Detector	0.10
TOTAL	0.033

If an InAs detector having an 0.50 quantum efficiency is used, the total optical efficiency becomes 0.164.

Aircraft Contamination

An added difficulty in trying to measure water is that most materials will experience some outgassing of water and potentially contaminate the experiment. Simple calculations were performed to examine whether outgassed water from the aircraft could interfere with any measurements being made from the plane.

When the diffusion of water vapor is considered by itself, it is found that at 15 km, where the mean free path of water vapor, λ is largest, any outgassing of water from the aircraft skin remains very close to the skin and will not readily contaminate any measurement.

More importantly is the effect of a transverse high altitude wind with a velocity v_T. Water vapor outgassed from the aircraft will be carried along by the wind a distance, $d = v_T t$ where $t = z/v_a$ and z is the distance from the tip of the aircraft to the station of the sensor.

The distance to the edge of the outgassed water cloud is

$$d = \frac{v_T z}{v_a}$$

using reasonable values

$$d = \frac{(6 \times 10^3 \ cm/s)(1220 \ cm)}{2.7 \times 10^4 \ cm/s} = 2.7 \times 10^2 \ cm$$

which is still much smaller than typical lidar ranges

Conventional Raman Scattering

Raman scattering is a technique that identifies target species by a unique scattering mechanism. The incident wavelength is absorbed by the molecule which is excited into a virtual state. The scattered wavelength is emitted with a wavelength that is different than the incident

photon and the molecule is left in some final state. Raman scattering is a useful method for identifying specific constituents from a mixture of gases. The vibrational-rotational cross sections for this phenomena are typically several orders of magnitude smaller than Rayleigh scattering.

Simulations of Raman scattered signals from water vapor have been made for the Nd:Yag wavelengths 532, 355, and 266 nanometers. The incident energy per pulse used for the lasers was 150, 30, and 80 mj, respectively. (N.B. The 266 nm power level was obtained from a laser catalog; the 532 and 355 nm wavelengths are based on laboratory measurements.) The results are directly proportional to the energy per pulse. Although the 532 nm wavelength has more incident power than the UV wavelengths, the combination of higher background, dark counts, and the λ^{-4} cross section dependence make it a smaller signal to noise ratio. The return signals have been integrated for 200 seconds at 10 pps (2000 shots coadded) with a sampling rate of 0.2 μs (30 meter bins) and are shown plotted in Fig. 3a-c. The long integration time is required to obtain a useful measurement. The data from these plots are also presented in tabular form in Appendix A.

The calculations show that measurements with adequate signal strength would be confined to a range of a kilometer at low altitudes, hundreds of meters from the aircraft around 5 km, and less than 100 meters above 10 km. The 266 nm signal is the strongest of the three wavelengths followed by the 355 nm signal; this is because of the strong λ^{-4} dependence of the cross section. The signal decreases rapidly for altitudes above 8 km due to the fall off of the mixing ratio. In all three cases the signal above 12 km is very weak even close to the aircraft where $1/r^2$ is rapidly increasing. Fig. 4 is a plot of range versus altitude for the different wavelengths. Each point on a curve represents a return signal of ~ 100 photoelectrons which is a statistically significant (10 percent) signal.

Differential Absorption

The differential absorption lidar technique (DIAL) is a measurement of the extinction term and is independent of β. Whereas measurements of Raman scattering are dependent on the

backscattering of photons, differential absorption measurements are dependent on what happens to the photons before and after backscattering. The extinction coefficient is separated into two terms

$$\tau = \kappa(\lambda,r)\, \delta r + N(r)\, \sigma(\lambda,r)$$

One term contains the effects from all atmospheric constituents except the species of interest and the other term is due to absorption exclusively by the target species. The target concentration is determined by comparing a measurement at a wavelength sensitive to the absorption with a second measurement very close in wavelength but insensitive to absorption by the target species. The two equations are solved for the density which is given below:

$$N(r) = \frac{1}{2[\sigma(\lambda_1,r) - \sigma(\lambda_2,r)]\ \delta r} \ln \frac{[P(\lambda_1,r)\ P(\lambda_2,r+\delta r)]}{[P(\lambda_1,r+\delta r)\ P(\lambda_2,r)]}$$

Choice of Absorption Line

There are hundreds of water absorption lines to choose from. Several criteria are used to determine the optimum line. The line should be chosen to be in an spectral region where other constituents (e.g. CO_2) do not interfere. It is desirable that the absorption cross section be independent of temperature, therefore, a ground state transition is desirable. The line should be chosen such that the extinction does not drive the exponential into saturation and is the most sensitive region of the exponential.

Laser Spectral Bandwidth

The equation derived for N(r) assumes that the laser is monochromatic. When the spectral bandwidth of the laser is narrow compared to the absorption peak this is a good approximation, however, when the laser bandwidth is wide (e.g. dye laser) or the absorption feature is respectively narrow, the amount of absorption must be integrated over the wavelength. This requires an accurate knowledge of the spectral shapes.

Simulations

DIAL returns for wavelengths "off" the absorption peak were calculated. The assumption is made that an appropriate absorption line can be found providing enough signal can be backscattered off the atmosphere. These calculations do not include background or detector noise. The calculations have been carried out for the altitudes or 2 ,5 ,7 ,10 ,12 ,and 14 km and have coadded 2000 shots in 30 meter bins for direct comparison with the Raman scattering data.

The calculations are made at 1.85 μm, a region where several suitable H_2O absorption lines are found (e.g. λ = 1.8549 μm, $\sigma = 1.55 \times 10^{-22}$ cm^2). A plot of the data is shown in Fig. 5; the same data is listed in a table in Appendix B. The return signals have good statistics out to 2 - 3 km at all altitudes. Note that the measurement at 2 km is less than the signal at 5 km at a range greater than ~270 meters. This is due to the peak in the backscatter mixing ratio seen in Fig. 1 and the increased extinction at the lower altitude.

The return signals at 1.85 μm are significantly larger than those due to Raman scattering. This is because of the small size of the Raman scattering cross section. The DIAL method generates 875 photoelectrons from a range of 2 km and an altitude of 14 km. At a range of 1000 meters, typical return signals are in excess of 10^6 photoelectrons at altitudes below 7 km and a few thousand counts up to 14 km. The above numbers do not include background or detector noise.

Detection at 1.85 μm can be done with a InAs detector cooled to LN_2 temperatures. The value for D* at this wavelength is ~ 10^{11} cm-Hz$^{1/2}$/W from which a NEP of ~3000 photons/bin is obtained. The natural background was assumed to be due to scattering from a 300 K blackbody. The 300 degree blackbody radiance at 1.85 μm is 9.5×10^{-9} Watts-cm^{-2}-μm. After folding in the system characteristics the blackbody contribution is negligible. The total background is therefore assumed to be detector noise.

When the background is considered, the signal at the lower altitudes still maintains good signal to noise out to ranges over a kilometer. In a worst case, the range is restricted to ~400 m at 14 km.

A suitable laser emitting at this wavelength is available from Schwartz Electro-Optics. The laser is a solid state laser using a Co:MgF_2 crystal for lasing (Nd:YAG pumped) and is

tunable over the range 1.75 to 2.5 μm. The laser can be Q-switched with a typical pulse energy of 20 mj and a pulse width of $\sim$100 ns (15 meters). The spectral bandwidth is $\sim$0.1 cm^{-1}, however other optics can be added to further reduce the width and still maintain the output power. This is because the output power is determined by the mirror damage threshold and the laser can be pumped harder until the damage threshold is reached. A reference for some of this work is found in the IEEE Quantum Electronics, Vol. QE 21, p 202, 1985.

The eyesafe characteristics make the above laser a viable candidate for airborne measurements.

Topographical Scatter

One possible way to extend the range of the measurement is to replace $\beta_{atmosphere}$ with the backscatter coefficient from a hard target. This would significantly increase the signal to noise ratio, however, range information would be sacrificed. This target might be in the form of a large area retroreflector mounted on the side of another aircraft. Retroreflector arrays with a typical reflector dimension of 150 μm are etched onto 0.060 inch thick alumina thus providing large area retroreflectors which are light and compact.

Summary and Recommendations

Preliminary sensitivity calculations have been made for detecting water vapor in the troposphere and show that it is feasible to make remote measurements from an aircraft. The concentration of water vapor covers a very large dynamic range ($x10^4$ over 0 - 15 km). Conventional Raman scattering at Nd:Yag wavelengths and differential absorption ($\lambda = 1.85\mu$m) detection mechanisms have been examined.

The results from Raman scattering show that the signals must be integrated for a large amount of time (e.g. 200 seconds) to obtain statistically significant measurements. The calculations show that measurements would be confined to a range of a kilometer at low altitudes, hundreds of meters from the aircraft around 5 km, and less than 100 meters above 10 km. Data regarding longer ranges must be inferred statistically. Scattering at the shorter wavelengths is favored because of the strong λ^{-4} dependence of the cross section.

The DIAL method is a more sensitive technique and therefore a more promising technique for an aircraft lidar. The DIAL technique is a more complicated experiment and requires measurements at a second wavelength. However, it is able to record measurements on the order of a couple of kilometers at lower altitudes (< 7 km) and typically 0.5 kilometer at the ' igher altitudes. The use of a hard scatterer can significantly enhance the SNR, but range information is sacrificed.

Based on the results of this study it is recommended that a preliminary engineering design for an airborne DIAL lidar be developed. Using the simulation tools developed for this study, the engineering design specification will be optimized and a preliminary flight test plan developed.

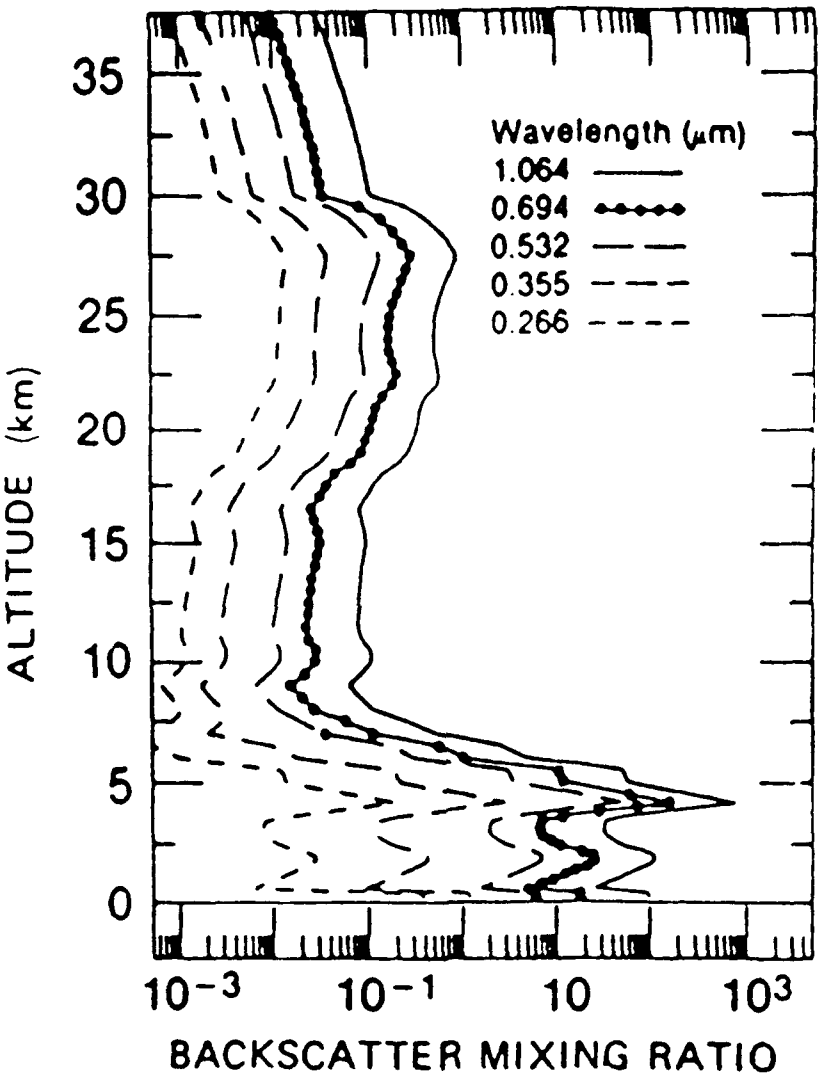

Figure 1.: Mixing ratio, $\beta_{Aerosol}/\beta_{Rayleigh}$ for various wavelengths (from Russell, P.B., B.M. Morley, J.M. Livingston, G.W. Grams, and E.M. Patterson, "Improved Simulation of Aerosol, Cloud, and Density Measurements by Shuttle Lidar", NASA Contractor Report 3473, NASA Langley Research Center, 1981)

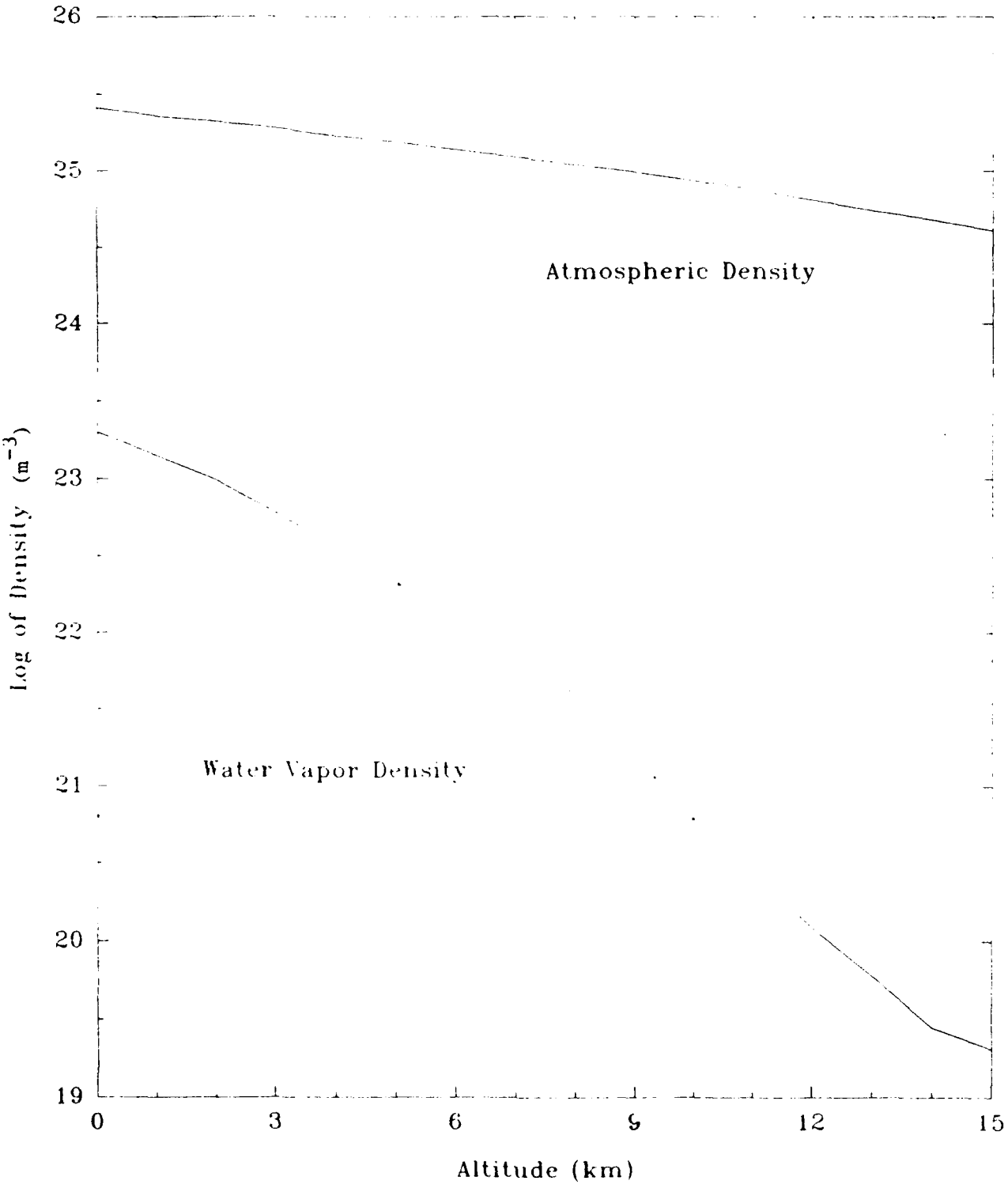

Figure 2.: Water Vapor Density

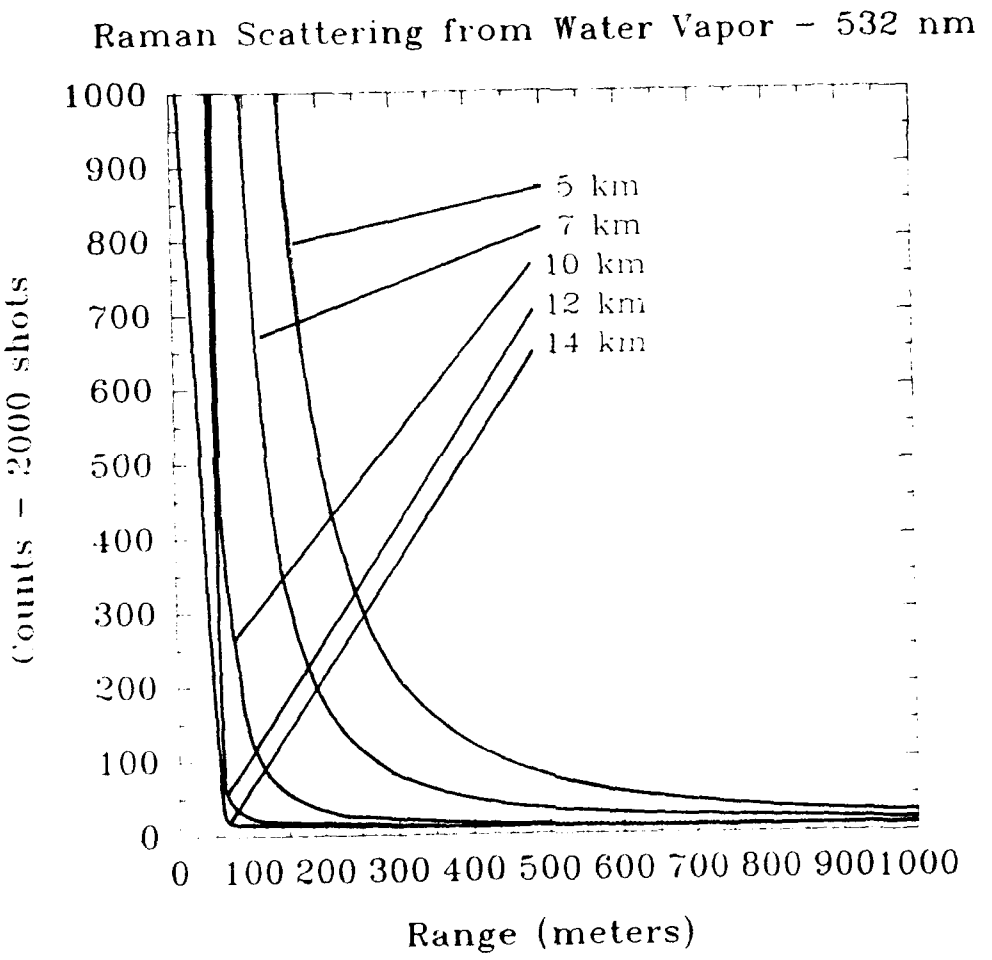

Figure 3a.: Raman scattering at 532 nm

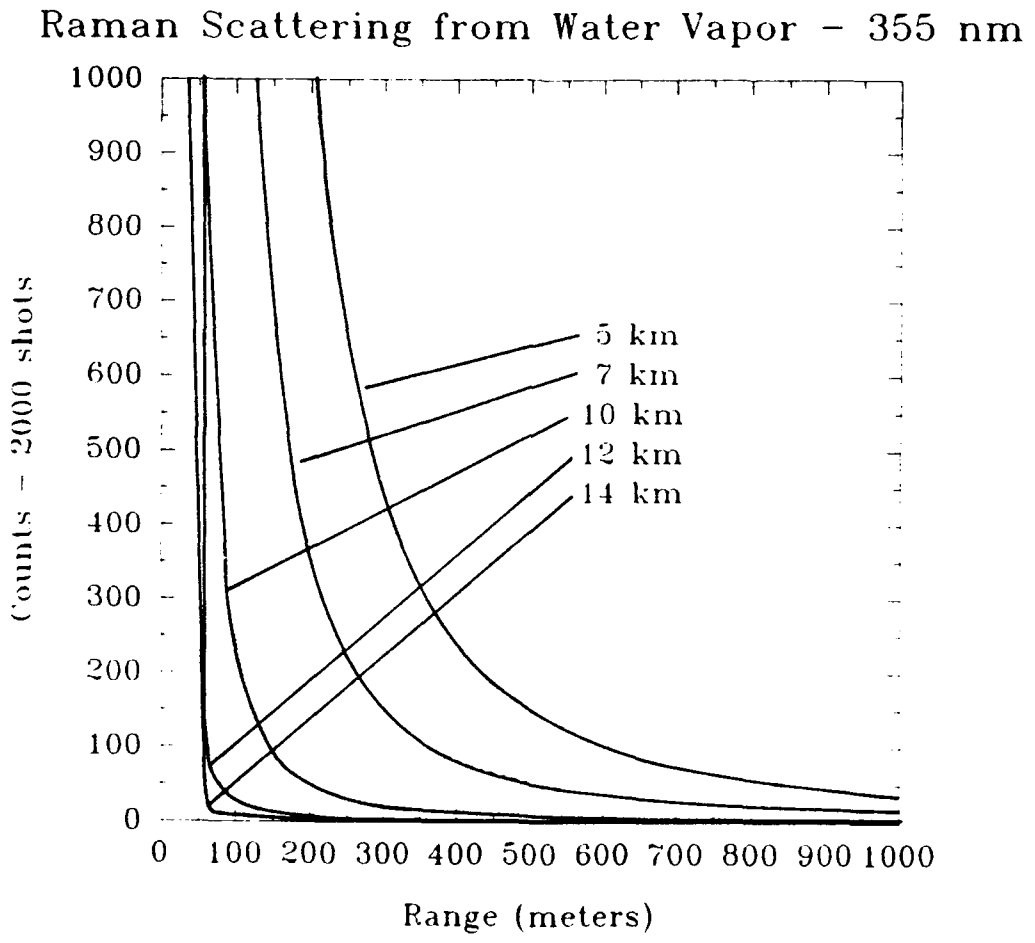

Figure 3b.: Raman scattering at 355 nm

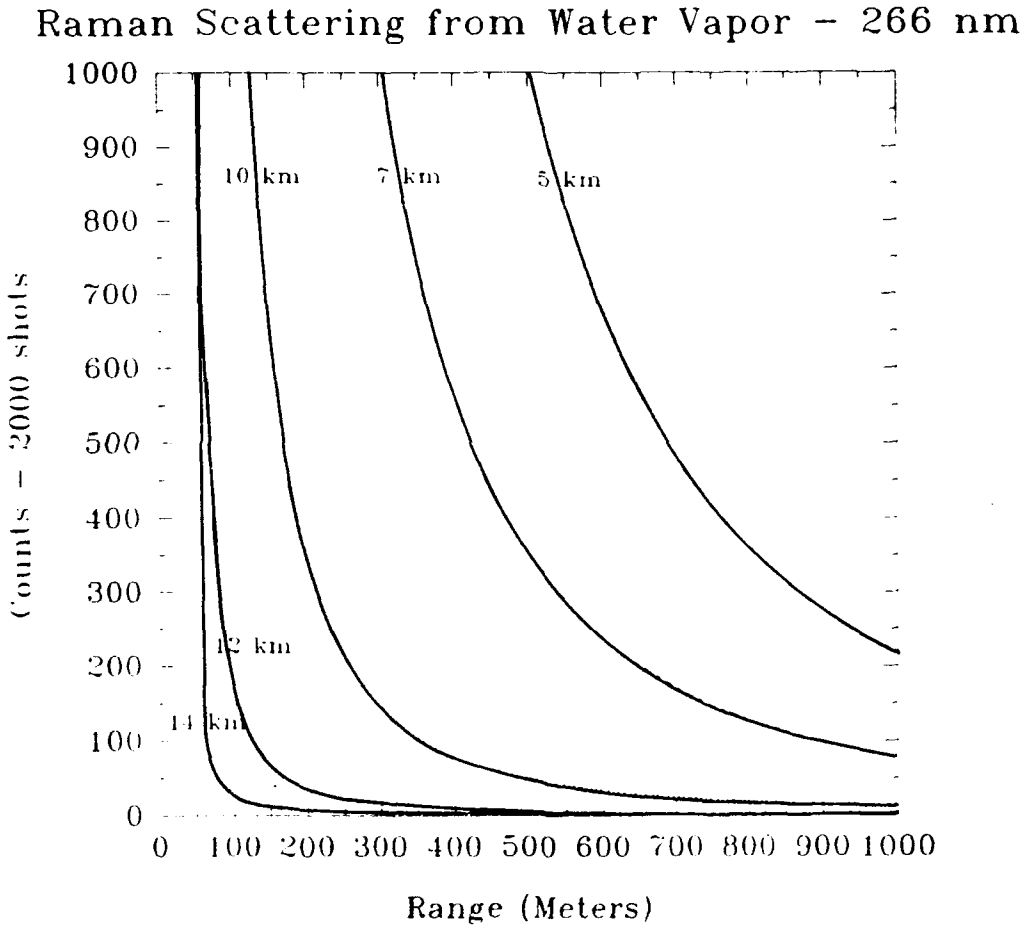

Figure 3c.: Raman scattering at 266 nm

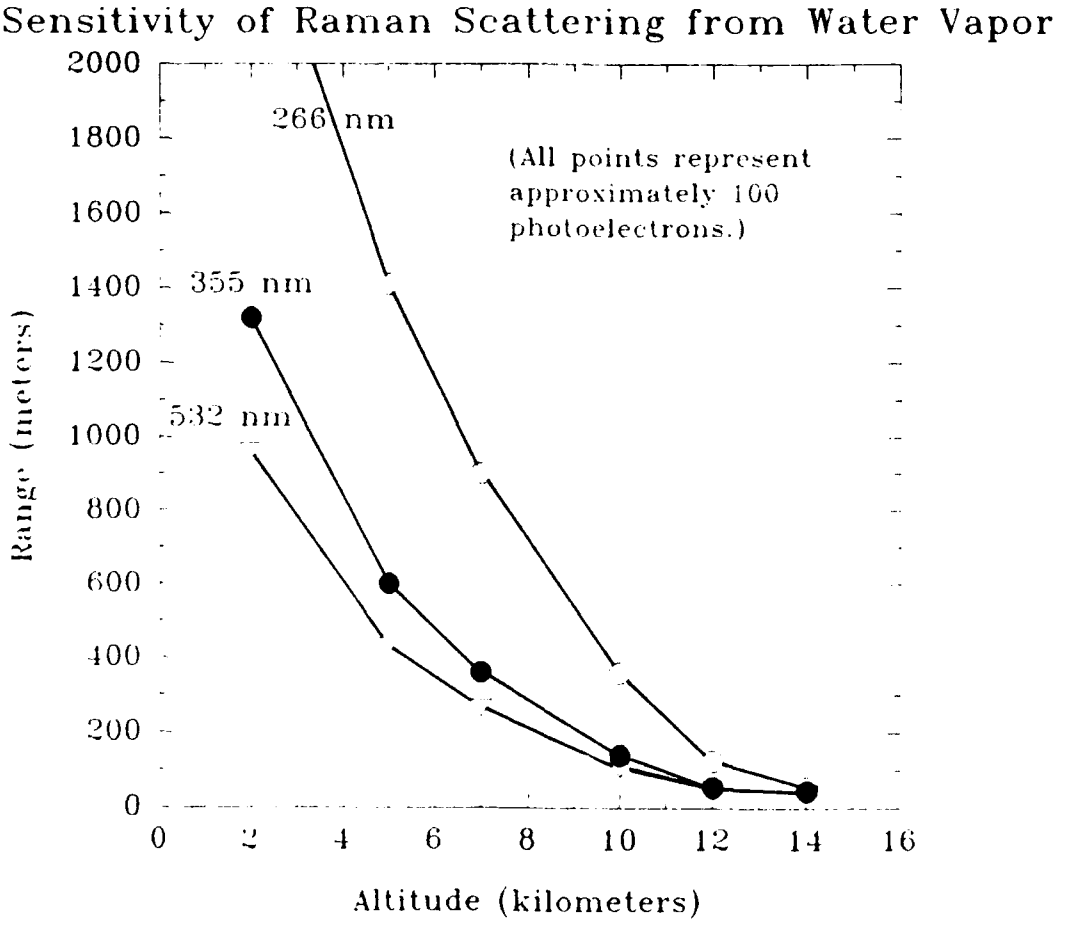

Figure 4.: Range versus altitude for constant Raman scattering returns

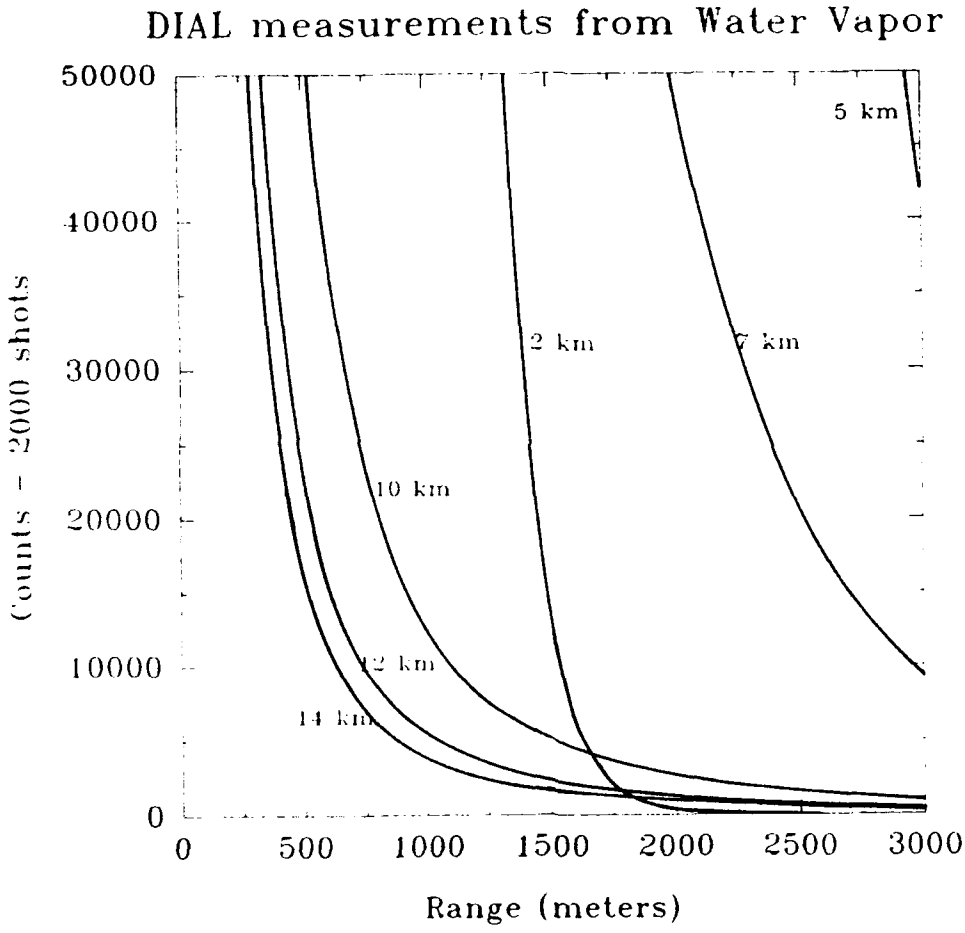

Figure 5.: DIAL "off peak" returns at $\lambda = 1.85\ \mu m$

Appendix A: Raman scattering returns at 532, 355, and 266 nm

Raman Scattering from Water Vapor (2000 shots) - 532 nm

Range (m)	2 km	5 km	7 km	10 km	12 km	14 km
30.0	5592990.0	913750.6	301834.0	40295.8	4062.9	579.6
60.0	55739.0	9176.5	3053.1	417.0	51.8	16.7
90.0	18618.5	3087.5	1036.0	147.8	24.7	12.9
120.0	9268.3	1549.5	525.4	79.6	17.8	11.9
150.0	5527.3	932.4	320.2	52.2	15.1	11.5
180.0	3660.5	623.7	217.4	38.5	13.7	11.3
210.0	2596.7	447.3	158.5	30.6	12.9	11.2
240.0	1934.2	337.2	121.6	25.7	12.4	11.1
270.0	1494.2	263.8	97.1	22.4	12.1	11.1
300.0	1187.4	212.5	79.8	20.1	11.9	11.1
330.0	965.2	175.3	67.3	18.5	11.7	11.0
360.0	799.2	147.4	57.9	17.2	11.6	11.0
390.0	672.1	126.0	50.7	16.2	11.5	11.0
420.0	572.7	109.2	45.0	15.5	11.4	11.0
450.0	493.5	95.7	40.5	14.9	11.3	11.0
480.0	429.5	84.9	36.8	14.4	11.3	11.0
510.0	377.0	75.9	33.7	14.0	11.2	11.0
540.0	333.4	68.5	31.2	13.6	11.2	11.0
570.0	296.9	62.2	29.0	13.4	11.2	11.0
600.0	266.0	56.9	27.2	13.1	11.1	11.0
630.0	239.7	52.4	25.7	12.9	11.1	11.0
660.0	217.0	48.5	24.3	12.7	11.1	11.0
690.0	197.5	45.1	23.2	12.6	11.1	11.0
720.0	180.4	42.1	22.1	12.4	11.1	11.0
750.0	165.4	39.5	21.2	12.3	11.1	10.9
780.0	152.3	37.2	20.4	12.2	11.1	10.9
810.0	140.7	35.2	19.7	12.1	11.0	10.9
840.0	130.3	33.3	19.1	12.0	11.0	10.9
870.0	121.1	31.7	18.5	11.9	11.0	10.9
900.0	112.8	30.3	18.0	11.9	11.0	10.9
930.0	105.4	28.9	17.6	11.8	11.0	10.9
960.0	98.7	27.7	17.2	11.8	11.0	10.9
990.0	92.7	26.7	16.8	11.7	11.0	10.9
1020.0	87.2	25.7	16.4	11.7	11.0	10.9
1050.0	82.2	24.8	16.1	11.6	11.0	10.9

Raman Scattering from Water Vapor (2000 shots) - 532 nm

Range (m)	2 km	5 km	7 km	10 km	12 km	14 km
1080.0	77.6	24.0	15.8	11.6	11.0	10.9
1110.0	73.4	23.2	15.6	11.5	11.0	10.9
1140.0	69.6	22.5	15.3	11.5	11.0	10.9
1170.0	66.1	21.9	15.1	11.5	11.0	10.9
1200.0	62.9	21.3	14.9	11.5	11.0	10.9
1230.0	59.9	20.7	14.7	11.4	11.0	10.9
1260.0	57.2	20.2	14.5	11.4	11.0	10.9
1290.0	54.6	19.8	14.3	11.4	11.0	10.9
1320.0	52.3	19.3	14.2	11.4	11.0	10.9
1350.0	50.1	18.9	14.0	11.3	11.0	10.9
1380.0	48.0	18.6	13.9	11.3	11.0	10.9
1410.0	46.1	18.2	13.8	11.3	11.0	10.9
1440.0	44.4	17.9	13.7	11.3	11.0	10.9
1470.0	42.7	17.6	13.5	11.3	11.0	10.9
1500.0	41.2	17.3	13.4	11.3	11.0	10.9
1530.0	39.7	17.0	13.3	11.3	11.0	10.9
1560.0	38.4	16.7	13.2	11.2	11.0	10.9
1590.0	37.1	16.5	13.2	11.2	11.0	10.9
1620.0	35.9	16.3	13.1	11.2	11.0	10.9
1650.0	34.8	16.1	13.0	11.2	11.0	10.9
1680.0	33.7	15.9	12.9	11.2	11.0	10.9
1710.0	32.7	15.7	12.9	11.2	11.0	10.9
1740.0	31.8	15.5	12.8	11.2	11.0	10.9
1770.0	30.9	15.3	12.7	11.2	11.0	10.9
1800.0	30.1	15.2	12.7	11.2	11.0	10.9
1830.0	29.3	15.0	12.6	11.2	11.0	10.9
1860.0	28.5	14.9	12.5	11.1	11.0	10.9
1890.0	27.8	14.7	12.5	11.1	11.0	10.9
1920.0	27.1	14.6	12.4	11.1	10.9	10.9
1950.0	26.5	14.5	12.4	11.1	10.9	10.9
1980.0	25.9	14.3	12.4	11.1	10.9	10.9
2010.0	25.3	14.2	12.3	11.1	10.9	10.9
2040.0	24.8	14.1	12.3	11.1	10.9	10.9
2070.0	24.2	14.0	12.2	11.1	10.9	10.9
2100.0	23.7	13.9	12.2	11.1	10.9	10.9

Raman Scattering from Water Vapor (2000 shots) - 532 nm

Range (m)	2 km	5 km	7 km	10 km	12 km	14 km
2130.0	23.3	13.8	12.2	11.1	10.9	10.9
2160.0	22.8	13.7	12.1	11.1	10.9	10.9
2190.0	22.4	13.6	12.1	11.1	10.9	10.9
2220.0	22.0	13.5	12.1	11.1	10.9	10.9
2250.0	21.6	13.5	12.0	11.1	10.9	10.9
2280.0	21.2	13.4	12.0	11.1	10.9	10.9
2310.0	20.9	13.3	12.0	11.1	10.9	10.9
2340.0	20.5	13.2	11.9	11.1	10.9	10.9
2370.0	20.2	13.2	11.9	11.1	10.9	10.9
2400.0	19.9	13.1	11.9	11.1	10.9	10.9
2430.0	19.6	13.1	11.9	11.1	10.9	10.9
2460.0	19.3	13.0	11.8	11.1	10.9	10.9
2490.0	19.0	12.9	11.8	11.0	10.9	10.9
2520.0	18.8	12.9	11.8	11.0	10.9	10.9
2550.0	18.5	12.8	11.8	11.0	10.9	10.9
2580.0	18.3	12.8	11.8	11.0	10.9	10.9
2610.0	18.0	12.7	11.7	11.0	10.9	10.9
2640.0	17.8	12.7	11.7	11.0	10.9	10.9
2670.0	17.6	12.6	11.7	11.0	10.9	10.9
2700.0	17.4	12.6	11.7	11.0	10.9	10.9
2730.0	17.2	12.5	11.7	11.0	10.9	10.9
2760.0	17.0	12.5	11.7	11.0	10.9	10.9
2790.0	16.8	12.5	11.6	11.0	10.9	10.9
2820.0	16.6	12.4	11.6	11.0	10.9	10.9
2850.0	16.5	12.4	11.6	11.0	10.9	10.9
2880.0	16.3	12.4	11.6	11.0	10.9	10.9
2910.0	16.1	12.3	11.6	11.0	10.9	10.9
2940.0	16.0	12.3	11.6	11.0	10.9	10.9
2970.0	15.8	12.3	11.6	11.0	10.9	10.9
3000.0	15.7	12.2	11.5	11.0	10.9	10.9

Raman Scattering from Water Vapor (2000 shots) - 355 nm

Range (m)	2 km	5 km	7 km	10 km	12 km	14 km
30.0	12090460.0	1974944.0	652278.4	87066.0	8760.1	1232.0
60.0	120814.5	19820.1	6566.9	879.6	91.2	15.4
90.0	40432.7	6656.9	2211.9	298.2	32.7	7.2
120.0	20161.2	3331.4	1110.4	151.0	17.9	5.1
150.0	12041.3	1997.1	667.9	91.9	12.0	4.3
180.0	7984.6	1329.3	446.2	62.3	9.0	3.8
210.0	5670.5	947.8	319.4	45.4	7.3	3.6
240.0	4227.5	709.5	240.1	34.8	6.2	3.5
270.0	3268.0	550.8	187.2	27.7	5.5	3.4
300.0	2598.2	439.8	150.2	22.7	5.0	3.3
330.0	2112.6	359.2	123.3	19.1	4.6	3.2
360.0	1749.5	298.8	103.2	16.4	4.4	3.2
390.0	1471.0	252.4	87.6	14.4	4.2	3.2
420.0	1253.0	216.1	75.5	12.7	4.0	3.1
450.0	1079.1	187.0	65.7	11.4	3.9	3.1
480.0	938.3	163.4	57.8	10.4	3.8	3.1
510.0	822.7	144.1	51.3	9.5	3.7	3.1
540.0	726.8	128.0	45.9	8.8	3.6	3.1
570.0	646.2	114.4	41.3	8.2	3.5	3.1
600.0	578.0	102.9	37.4	7.6	3.5	3.1
630.0	519.8	93.1	34.1	7.2	3.4	3.1
660.0	469.6	84.6	31.2	6.8	3.4	3.1
690.0	426.2	77.2	28.7	6.5	3.4	3.1
720.0	388.3	70.8	26.6	6.2	3.3	3.1
750.0	355.1	65.1	24.6	5.9	3.3	3.1
780.0	325.8	60.2	23.0	5.7	3.3	3.0
810.0	299.8	55.7	21.5	5.5	3.3	3.0
840.0	276.8	51.8	20.1	5.3	3.2	3.0
870.0	256.2	48.3	18.9	5.2	3.2	3.0
900.0	237.7	45.1	17.8	5.0	3.2	3.0
930.0	221.1	42.2	16.8	4.9	3.2	3.0
960.0	206.0	39.7	16.0	4.8	3.2	3.0
990.0	192.4	37.3	15.2	4.7	3.2	3.0
1020.0	180.1	35.2	14.4	4.6	3.2	3.0
1050.0	168.8	33.2	13.8	4.5	3.2	3.0

Raman Scattering from Water Vapor (2000 shots) - 355 nm

Range (m)	2 km	5 km	7 km	10 km	12 km	14 km
1080.0	158.6	31.4	13.1	4.4	3.1	3.0
1110.0	149.2	29.8	12.6	4.3	3.1	3.0
1140.0	140.5	28.3	12.1	4.2	3.1	3.0
1170.0	132.6	26.9	11.6	4.2	3.1	3.0
1200.0	125.3	25.6	11.2	4.1	3.1	3.0
1230.0	118.5	24.5	10.7	4.1	3.1	3.0
1260.0	112.3	23.4	10.4	4.0	3.1	3.0
1290.0	106.5	22.3	10.0	4.0	3.1	3.0
1320.0	101.1	21.4	9.7	3.9	3.1	3.0
1350.0	96.1	20.5	9.4	3.9	3.1	3.0
1380.0	91.5	19.7	9.1	3.8	3.1	3.0
1410.0	87.1	18.9	8.8	3.8	3.1	3.0
1440.0	83.1	18.2	8.6	3.8	3.1	3.0
1470.0	79.3	17.5	8.3	3.7	3.1	3.0
1500.0	75.7	16.9	8.1	3.7	3.1	3.0
1530.0	72.4	16.3	7.9	3.7	3.1	3.0
1560.0	69.3	15.8	7.7	3.7	3.1	3.0
1590.0	66.3	15.2	7.5	3.6	3.1	3.0
1620.0	63.6	14.7	7.4	3.6	3.1	3.0
1650.0	61.0	14.3	7.2	3.6	3.1	3.0
1680.0	58.5	13.8	7.0	3.6	3.1	3.0
1710.0	56.2	13.4	6.9	3.5	3.1	3.0
1740.0	54.0	13.0	6.7	3.5	3.1	3.0
1770.0	52.0	12.6	6.6	3.5	3.1	3.0
1800.0	50.0	12.3	6.5	3.5	3.1	3.0
1830.0	48.2	11.9	6.4	3.5	3.1	3.0
1860.0	46.4	11.6	6.3	3.5	3.1	3.0
1890.0	44.7	11.3	6.2	3.4	3.1	3.0
1920.0	43.2	11.0	6.0	3.4	3.1	3.0
1950.0	41.7	10.8	6.0	3.4	3.1	3.0
1980.0	40.2	10.5	5.9	3.4	3.0	3.0
2010.0	38.9	10.2	5.8	3.4	3.0	3.0
2040.0	37.6	10.0	5.7	3.4	3.0	3.0
2070.0	36.4	9.8	5.6	3.4	3.0	3.0
2100.0	35.2	9.6	5.5	3.4	3.0	3.0

Raman Scattering from Water Vapor (2000 shots) - 355 nm

Range (m)	2 km	5 km	7 km	10 km	12 km	14 km
2130.0	34.1	9.4	5.4	3.3	3.0	3.0
2160.0	33.0	9.2	5.4	3.3	3.0	3.0
2190.0	32.0	9.0	5.3	3.3	3.0	3.0
2220.0	31.0	8.8	5.2	3.3	3.0	3.0
2250.0	30.1	8.6	5.2	3.3	3.0	3.0
2280.0	29.2	8.4	5.1	3.3	3.0	3.0
2310.0	28.3	8.3	5.1	3.3	3.0	3 0
2340.0	27.5	8.1	5.0	3.3	3.0	3.0
2370.0	26.7	8.0	5.0	3.3	3.0	3.0
2400.0	26.0	7.8	4.9	3.3	3.0	3.0
2430.0	25.3	7.7	4.9	3.3	3.0	3.0
2460.0	24.6	7.6	4.8	3.3	3.0	3.0
2490.0	23.9	7.4	4.8	3.3	3.0	3.0
2520.0	23.3	7.3	4.7	3.2	3.0	3.0
2550.0	22.7	7.2	4.7	3.2	3.0	3.0
2580.0	22.1	7.1	4.6	3.2	3.0	3.0
2610.0	21.5	7.0	4.6	3.2	3.0	3.0
2640.0	21.0	6.9	4.6	3.2	3.0	3.0
2670.0	20.4	6.8	4.5	3.2	3.0	3.0
2700.0	19.9	6.7	4.5	3.2	3.0	3.0
2730.0	19.4	6.6	4.4	3.2	3.0	3.0
2760.0	19.0	6.5	4.4	3.2	3.0	3.0
2790.0	18.5	6.4	4.4	3.2	3.0	3.0
2820.0	18.1	6.3	4.4	3.2	3.0	3.0
2850.0	17.7	6.2	4.3	3.2	3.0	3.0
2880.0	17.3	6.2	4.3	3.2	3.0	3.0
2910.0	16.9	6.1	4.3	3.2	3.0	3.0
2940.0	16.5	6.0	4.2	3.2	3.0	3.0
2970.0	16.1	5.9	4.2	3.2	3.0	3.0
3000.0	15.8	5.9	4.2	3.2	3.0	3.0

Raman Scattering from Water Vapor (2000 shots) - 266 nm

Range (m)	2 km	5 km	7 km	10 km	12 km	14 km
30.0	88461000.0	14451000.0	4773000.0	637130.0	64090.0	8996.0
60.0	878190.0	144270.0	47811.0	6396.1	645.5	92.0
90.0	292380.0	48249.0	16032.0	2149.0	218.0	32.0
120.0	145050.0	24041.0	8009.5	1075.9	110.0	16.8
150.0	86194.0	14348.0	4792.8	645.3	66.6	10.7
180.0	56866.0	9507.0	3184.1	429.8	44.8	7.7
210.0	40180.0	6746.6	2265.6	306.7	32.4	5.9
240.0	29802.0	5025.8	1692.3	229.8	24.7	4.8
270.0	22920.0	3882.1	1310.7	178.5	19.5	4.1
300.0	18129.0	3084.0	1044.1	142.7	15.9	3.6
330.0	14604.0	2505.5	850.6	116.7	13.3	3.2
360.0	12081.0	2073.1	705.7	97.2	11.3	2.9
390.0	10105.0	1741.7	594.6	82.2	9.8	2.7
420.0	8562.1	1482.2	507.4	70.5	8.6	2.6
450.0	7335.1	1275.4	437.9	61.1	7.6	2.4
480.0	6344.2	1108.0	381.5	53.5	6.9	2.3
510.0	5533.3	970.6	335.2	47.2	6.2	2.2
540.0	4861.7	856.6	296.7	42.0	5.7	2.2
570.0	4299.6	761.0	264.3	37.6	5.3	2.1
600.0	3824.9	680.0	236.9	33.9	4.9	2.0
630.0	3420.6	610.8	213.4	30.7	4.6	2.0
660.0	3073.6	551.3	193.2	28.0	4.3	2.0
690.0	2773.9	499.8	175.7	25.6	4.0	1.9
720.0	2513.3	454.9	160.4	23.5	3.8	1.9
750.0	2285.4	415.5	147.0	21.7	3.6	1.9
780.0	2085.2	380.9	135.1	20.1	3.5	1.8
810.0	1908.4	350.1	124.6	18.7	3.3	1.8
840.0	1751.5	322.8	115.3	17.4	3.2	1.8
870.0	1611.9	298.5	106.9	16.2	3.1	1.8
900.0	1487.0	276.6	99.4	15.2	3.0	1.8
930.0	1375.0	256.9	92.6	14.3	2.9	1.8
960.0	1274.1	239.2	86.5	13.5	2.8	1.7
990.0	1183.0	223.1	81.0	12.7	2.7	1.7
1020.0	1100.6	208.5	75.9	12.0	2.6	1.7
1050.0	1025.7	195.3	71.3	11.4	2.6	1.7

Raman Scattering from Water Vapor (2000 shots) - 266 nm

Range (m)	2 km	5 km	7 km	10 km	12 km	14 km
1080.0	957.5	183.1	67.1	10.8	2.5	1.7
1110.0	895.3	172.0	63.3	10.3	2.5	1.7
1140.0	838.3	161.9	59.8	9.8	2.4	1.7
1170.0	786.2	152.5	56.5	9.3	2.4	1.7
1200.0	738.2	143.9	53.5	8.9	2.3	1.7
1230.0	694.1	135.9	50.7	8.5	2.3	1.7
1260.0	653.4	128.6	48.1	8.2	2.3	1.7
1290.0	615.9	121.8	45.8	7.8	2.2	1.7
1320.0	581.1	115.5	43.5	7.5	2.2	1.7
1350.0	548.9	109.6	41.5	7.3	2.2	1.7
1380.0	519.0	104.1	39.5	7.0	2.1	1.7
1410.0	491.1	99.0	37.8	6.7	2.1	1.6
1440.0	465.3	94.3	36.1	6.5	2.1	1.6
1470.0	441.1	89.8	34.5	6.3	2.1	1.6
1500.0	418.6	85.6	33.0	6.1	2.0	1.6
1530.0	397.6	81.7	31.6	5.9	2.0	1.6
1560.0	377.9	78.1	30.3	5.7	2.0	1.6
1590.0	359.5	74.7	29.1	5.5	2.0	1.6
1620.0	342.2	71.4	28.0	5.4	2.0	1.6
1650.0	326.0	68.4	26.9	5.2	2.0	1.6
1680.0	310.7	65.5	25.9	5.1	1.9	1.6
1710.0	296.4	62.8	24.9	5.0	1.9	1.6
1740.0	282.9	60.3	24.0	4.8	1.9	1.6
1770.0	270.2	57.8	23.1	4.7	1.9	1.6
1800.0	258.2	55.6	22.3	4.6	1.9	1.6
1830.0	246.9	53.4	21.5	4.5	1.9	1.6
1860.0	236.2	51.3	20.8	4.4	1.9	1.6
1890.0	226.1	49.4	20.1	4.3	1.9	1.6
1920.0	216.5	47.6	19.4	4.2	1.8	1.6
1950.0	207.5	45.8	18.8	4.1	1.8	1.6
1980.0	198.9	44.2	18.2	4.0	1.8	1.6
2010.0	190.8	42.6	17.6	3.9	1.8	1.6
2040.0	183.1	41.1	17.0	3.9	1.8	1.6
2070.0	175.8	39.6	16.5	3.8	1.8	1.6
2100.0	168.8	38.3	16.0	3.7	1.8	1.6

Raman Scattering from Water Vapor (2000 shots) - 266 nm

Range (m)	2 km	5 km	7 km	10 km	12 km	14 km
2130.0	162.2	37.0	15.5	3.6	1.8	1.6
2160.0	155.9	35.7	15.1	3.6	1.8	1.6
2190.0	149.9	34.6	14.6	3.5	1.8	1.6
2220.0	144.2	33.4	14.2	3.5	1.8	1.6
2250.0	138.8	32.3	13.8	3.4	1.8	1.6
2280.0	133.6	31.3	13.4	3.3	1.8	1.6
2310.0	128.7	30.3	13.1	3.3	1.8	1.6
2340.0	124.0	29.4	12.7	3.2	1.7	1.6
2370.0	119.5	28.5	12.4	3.2	1.7	1.6
2400.0	115.2	27.6	12.1	3.1	1.7	1.6
2430.0	111.1	26.8	11.8	3.1	1.7	1.6
2460.0	107.2	26.0	11.5	3.1	1.7	1.6
2490.0	103.4	25.2	11.2	3.0	1.7	1.6
2520.0	99.8	24.5	10.9	3.0	1.7	1.6
2550.0	96.4	23.8	10.6	2.9	1.7	1.6
2580.0	93.1	23.1	10.4	2.9	1.7	1.6
2610.0	90.0	22.4	10.1	2.9	1.7	1.6
2640.0	86.9	21.8	9.9	2.8	1.7	1.6
2670.0	84.0	21.2	9.7	2.8	1.7	1.6
2700.0	81.3	20.6	9.5	2.8	1.7	1.6
2730.0	78.6	20.1	9.2	2.7	1.7	1.6
2760.0	76.1	19.5	9.0	2.7	1.7	1.6
2790.0	73.6	19.0	8.8	2.7	1.7	1.6
2820.0	71.2	18.5	8.6	2.7	1.7	1.6
2850.0	69.0	18.0	8.5	2.6	1.7	1.6
2880.0	66.8	17.6	8.3	2.6	1.7	1.6
2910.0	64.7	17.1	8.1	2.6	1.7	1.6
2940.0	62.7	16.7	8.0	2.6	1.7	1.6
2970.0	60.8	16.3	7.8	2.5	1.7	1.6
3000.0	58.9	15.9	7.6	2.5	1.7	1.6

Appendix B: DIAL "off peak" returns at 1.85 μm

DIAL Technique from Water Vapor (2000 shots) - 1.85 μm

Range (m)	2 km	5 km	7 km	10 km	12 km	14 km
30	2.0735e+013	6.8351e+012	5.7009e+010	7.6564e+008	2.9382e+008	2.0716e+008
60	1.6248e+011	6.3784e+010	5.5574e+008	7.6713e+006	2.9562e+006	2.0871e+006
90	4.4822e+010	2.022e+010	1.8238e+008	2.5727e+006	994650	703010
120	1.8512e+010	9.5631e+009	8.9215e+007	1.2854e+006	498560	352750
150	9.1722e+009	5.4197e+009	5.2281e+007	769250	299300	211980
180	5.0489e+009	3.4107e+009	3.4016e+007	511080	199480	141430
210	2.9776e+009	2.299e+009	2.3704e+007	363650	142380	101050
240	1.8438e+009	1.6268e+009	1.734e+007	271620	106680	75796
270	1.184e+009	1.1937e+009	1.3152e+007	210360	82880	58946
300	7.8205e+008	9.0079e+008	1.026e+007	167550	66221	47147
330	5.2828e+008	6.9519e+008	8.1852e+006	136480	54109	38564
360	3.6347e+008	5.4643e+008	6.6505e+006	113220	45029	32125
390	2.5392e+008	4.3609e+008	5.4865e+006	95365	38047	27172
420	1.7969e+008	3.5255e+008	4.5849e+006	81366	32564	23280
450	1.2857e+008	2.8817e+008	3.8739e+006	70192	28180	20167
480	9.2882e+007	2.3781e+008	3.3045e+006	61134	24620	17638
510	6.7663e+007	1.979e+008	2.8425e+006	53691	21690	15555
540	4.9656e+007	1.659e+008	2.4632e+006	47503	19251	13820
570	3.6681e+007	1.3999e+008	2.1485e+006	42304	17197	12358
600	2.7256e+007	1.1882e+008	1.885e+006	37895	15453	11117
630	2.036e+007	1.0139e+008	1.6626e+006	34125	13960	10052
660	1.5281e+007	8.6925e+007	1.4734e+006	30877	12670	9133.5
690	1.1519e+007	7.4848e+007	1.3114e+006	28059	11550	8334.7
720	8.7175e+006	6.4705e+007	1.1719e+006	25599	10571	7635.8
750	6.6214e+006	5.614e+007	1.051e+006	23440	9709.6	7020.9
780	5.0461e+006	4.8871e+007	945690	21535	8948.3	6477.2
810	3.8575e+006	4.2675e+007	853580	19846	8271.1	5993.9
840	2.9573e+006	3.737e+007	772650	18341	7668.8	5562.5
870	2.2731e+006	3.2812e+007	701240	16995	7128.4	5175.9
900	1.7516e+006	2.8881e+007	638000	15787	6642.4	4828
930	1.3528e+006	2.5479e+007	581800	14698	6203.8	4513.8
960	1.0471e+006	2.2526e+007	531690	13714	5806.6	4229.2
990	812080	1.9956e+007	486880	12822	5445.8	3970.5
1020	631010	1.7713e+007	446690	12011	5117.1	3734.7
1050	491200	1.5749e+007	410550	11270	4816.8	3519.2

DIAL Technique from Water Vapor (2000 shots) - 1.85 μm

Range (m)	2 km	5 km	7 km	10 km	12 km	14 km
1080	383000	1.4027e+007	377960	10594	4541.8	3321.7
1110	299110	1.2513e+007	348520	9973.5	4289.3	3140.3
1140	233950	1.118e+007	321850	9403.6	4056.9	2973.2
1170	183250	1.0002e+007	297650	8879	3842.5	2819
1200	143720	8.9608e+006	275640	8394.9	3644.4	2676.5
1230	112870	8.0382e+006	255580	7947.4	3461	2544.4
1260	88748	7.2194e+006	237280	7533	3290.8	2421.7
1290	69863	6.4916e+006	220540	7148.4	3132.6	2307.7
1320	55058	5.8435e+006	205200	6791	2985.3	2201.5
1350	43436	5.2658e+006	191140	6458.3	2847.9	2102.3
1380	34302	4.7499e+006	178220	6148.1	2719.6	2009.7
1410	27115	4.2888e+006	166330	5858.5	2599.6	1923
1440	21454	3.876e+006	155380	5587.6	2487.2	1841.7
1470	16990	3.506e+006	145280	5334	2381.7	1765.5
1500	13466	3.174e+006	135950	5096.3	2282.7	1693.8
1530	10682	2.8758e+006	127330	4873.1	2189.6	1626.4
1560	8479.6	2.6077e+006	119340	4663.3	2101.9	1562.9
1590	6736.7	2.3664e+006	111940	4466	2019.2	1503
1620	5355.9	2.1489e+006	105080	4280.1	1941.3	1446.4
1650	4261.1	1.9528e+006	98705	4104.8	1867.6	1393
1680	3392.4	1.7758e+006	92779	3939.3	1797.9	1342.4
1710	2702.5	1.6159e+006	87266	3783	1732	1294.5
1740	2154.3	1.4713e+006	82132	3635.1	1669.5	1249.1
1770	1718.3	1.3405e+006	77346	3495.2	1610.2	1206
1800	1371.4	1.222e+006	72883	3362.6	1554	1165.1
1830	1095.1	1.1146e+006	68715	3236.8	1500.6	1126.2
1860	874.95	1.0172e+006	64821	3117.5	1449.8	1089.2
1890	699.44	928780	61180	3004.1	1401.4	1054
1920	559.42	848500	57774	2896.4	1355.4	1020.4
1950	447.65	775550	54584	2793.8	1311.5	988.39
1980	358.39	709200	51595	2696.3	1269.7	957.84
2010	287.06	648840	48792	2603.3	1229.7	928.67
2040	230.03	593880	46163	2514.7	1191.6	900.8
2070	184.41	543820	43694	2430.2	1155.1	874.15
2100	147.9	498190	41374	2349.5	1120.3	848.65

DIAL Technique from Water Vapor (2000 shots) - 1.85 μm

Range (m)	2 km	5 km	7 km	10 km	12 km	14 km
2130	118.67	456580	39195	2272.4	1086.9	824.23
2160	95.252	418610	37145	2198.7	1055	800.84
2190	76.486	383950	35216	2128.3	1024.4	778.41
2220	61.441	352300	33400	2060.9	995.05	756.91
2250	49.374	323370	31690	1996.4	966.92	736.27
2280	39.691	296930	30077	1934.6	939.91	716.44
2310	31.918	272740	28557	1875.3	913.99	697.4
2340	25.676	250610	27123	1818.5	889.08	679.1
2370	20.662	230350	25770	1764	865.14	661.49
2400	16.632	211800	24491	1711.7	842.11	644.56
2430	13.393	194800	23284	1661.5	819.96	628.25
2460	10.788	179230	22143	1613.2	798.64	612.55
2490	8.6917	164950	21064	1566.8	778.11	597.41
2520	7.0051	151850	20044	1522.2	758.32	582.83
2550	5.6474	139830	19079	1479.3	739.25	568.76
2580	4.5541	128800	18165	1438	720.87	555.19
2610	3.6735	118670	17300	1398.3	703.13	542.09
2640	2.964	109370	16480	1360	686.01	529.44
2670	2.3921	100820	15703	1323.1	669.49	517.22
2700	1.931	92962	14967	1287.5	653.53	505.41
2730	1.5593	85740	14269	1253.2	638.1	493.99
2760	1.2594	79099	13606	1220.1	623.2	482.95
2790	1.0174	72989	12978	1188.2	608.79	472.27
2820	0.82209	67367	12381	1157.3	594.85	461.94
2850	0.66443	62192	11815	1127.5	581.36	451.93
2880	0.53714	57428	11277	1098.8	568.31	442.24
2910	0.43432	53040	10766	1071	555.67	432.85
2940	0.35126	48998	10280	1044.1	543.43	423.75
2970	0.28415	45273	9818	1018.2	531.57	414.93
3000	0.2299	41841	9378.9	993.03	520.07	406.38